JOURNAL OF MATERIALS SCIENCE 31 (1996) 3073–3080

Preparation of small copper particles of high catalytic activity using a rotating cryostat

B. MILE*
School of Chemistry, University of Bristol, Cantock Close, Bristol B58 ITS, UK

J. A. HOWARD, M. TOMIETTO
Steacie Institute for Molecular Sciences, National Research Council of Canada, Ottawa, Ontario, Canada K1A 0R6

H. A. JOLY
Department of Chemistry, Laurentian University, Sudbury, Ontario, Canada P3E 2C6

A. SAYARI
Department of Chemical Engineering and CERPIC, Université Laval, Quebec City, Quebec, Canada G1K 7P4

The rotating cryostat technique was used to trap small naked copper clusters, Cu_n, $n=3$–7, and the copper carbonyls $Cu_n(CO)_m$, $n=1$–2, $m=1$–6 in adamantane at 77 K. These clusters and carbonyls were then released from the adamantane for incorporation into inert supports (Al_2O_3 and SiO_2) at low temperatures (110 K) by slowly dissolving the host adamantane matrix into an isopentane containing a slurry of the support. Highly active catalysts for CO oxidation and CO/H_2 conversion to alkanes, alkenes and alcohols and with virtually unit dispersion were produced in this way. Efficient catalytic materials were also produced by directly implanting copper atoms into previously evaporated and condensed sodium chloride layers. In this system the copper was embedded in nanocrystals of the halide of <8 nm diameter.

1. Introduction

Ultra-fine particles can be prepared by quenching vapours emanating from high-temperature furnaces into condensed "inert"substrates at cryogenic temperatures [1–9]: the so-called SMAD technique (solvated metal atom dispersion). They have unusual magnetic properties [2], show quantum-size effects [8, 9], and high chemical activity [1–4]. Highly dispersed particles of metals such as platinum have also been prepared on inert supports by complexing the vapour-deposited metal atoms with ligands such as ethylene which are so weakly bound that the metal atoms can be released to form very small aggregates or clusters on the surface of the supports at very low temperatures [4]. Epitaxial deposition of metals on to previously deposited alkali halide layers gives highly active materials which show marked effects on the underlying substrates, on the preferred growth of certain metal crystal faces and hence on their activity for reactions such as alkane hydrogenolysis [10, 11]. These methods provide alternatives to the traditional ways of preparing supported metal catalysts which are multistage processes in which the metal particles are generated only at the final stage usually by reduction of a precursor metal oxide with hydrogen at high temperatures.

Using the rotating cryostat technique [12–16] we have been able to make and characterize several small naked metal clusters. M_n ($n = 3$ and 7), in the globular hydrocarbon adamantane and found them to persist in this matrix up to ambient temperatures [14–16]. We have also found that the carbonyls of copper, namely $Cu(CO)_3$ and $Cu_2(CO)_6$, are also stable to 273 K in adamantane [17, 18]. Here we report our attempts to take advantage of this unexpected stability by using copper clusters and carbonyls prepared in adamantane to fabricate highly dispersed metal particles on inert supports and to examine their catalytic activity for CO oxidation and for Fischer-Tropsch and methanol synthesis. We also describe the preparation and activity of copper atoms and particles in sodium chloride nanocrystals, prepared by direct implantation of copper vapour into previously deposited halide layers.

*Author to whom all correspondence should be addressed.

0022–2461

2. Experimental procedure

2.1. The rotating cryostat technique

This technique is a molecular engineering device for the rapid mixing [12–16], at the molecular level, of materials that are normally immiscible. Its principle is illustrated in Fig. 1. Vapours of the materials are condensed sequentially on to the cold surface of a stainless steel drum (12 cm o.d.) containing liquid nitrogen and spinning at ~2000 r.p.m. in an evacuated chamber ($< 10^{-6}$ torr; 1 torr = 133.322 Pa). Interleaving spirals of the layered materials develop until, after some 20 min, a deposit ~1 cm wide and several millimetres thick is formed with the thickness of each layer per revolution, being variable but controllable from submonolayer to 1–20 monolayers. The most important differences compared with static and slowly moving cryostats are:

(i) the large area of ~2000 cm^2 exposed for deposition per second compared with the ~1 cm^2 area available in other devices;

(ii) each material is condensed separately on to the top of a cold frozen layer of the previously deposited material, not into an ill-defined "slush" which is often encountered in static devices. The deposits can be examined by *in situ* reflectance Fourier transform–infrared (FT–IR) and UV/visible spectroscopies or by electron paramagnetic resonance (EPR) and NMR spectroscopies after transfer from the drum at 77 K and still under high vacuum. They can also be processed further for catalytic or other uses after transfer;

(iii) great advantage accrues from the rapid movement of the drum surface past the hot furnace sources (dimensions ~1 cm) of the metals. The cold surface is exposed to the high temperatures of the furnaces (up to 2800 K) placed a few millimetres away for only milliseconds. As a result, no matrix pyrolysis or annealing occurs and much higher deposition rates can be used than in most other matrix isolation or molecular beam epitaxial growth methods.

2.2. Preparation of supported copper particles and catalysts

We have used three methods for preparing copper catalysts on oxide and other supports: (i) copper clusters in adamantane dissolved at 110 K into isopentane containing suspensions of the Al_2O_3 or SiO_2 supports, (ii) copper carbonyls, $Cu(CO)_3$ and $Cu_2(CO)_6$, in adamantane dissolved at 110 K into isopentane containing suspensions of Al_2O_3 or SiO_2; (iii) direct implantation of copper vapours into sodium chloride layers previously condensed from a preceding oven source.

2.2.1. Copper clusters in adamantane

Ten monolayers of adamantane were deposited per revolution of the cold drum and copper vapourized from a resistively heated molybdenum furnace at ~1500 K was deposited to give about one-tenth of a monolayer per revolution. This gave a sample containing Cu_3 and Cu_7 and higher clusters as shown by EPR [14–16]. At the end of the experiment, samples containing about 5 mg copper clusters in about 1 g adamantane were transferred from the drum still at 77 K and 10^{-6} torr (see [12] for a detailed description), on to 5 ml frozen isopentane into which 50 mg Al_2O_3 or SiO_2 had been dispersed. The isopentane adamantane deposit was annealed slowly with vigorous agitation to 110 K (the melting point of isopentane) and then maintained at this temperature with agitation for 1 h. Subsequently, the sample was brought up to room temperature while being shaken thoroughly in two stages; 1 h at 193 K and 1 h at 273 K. The adamantane slowly dissolved in the isopentane to release the copper clusters so that they could be incorporated and anchored on to the surface of the support through oxide and hydroxyl groups. The hydrocarbons were then pumped from the support at room temperature. Adamantane was used as the carrier matrix rather than isopentane itself because we have found that higher yields of small clusters result in this plastic solid matrix and that they remain isolated to much higher temperature than in other matrices.

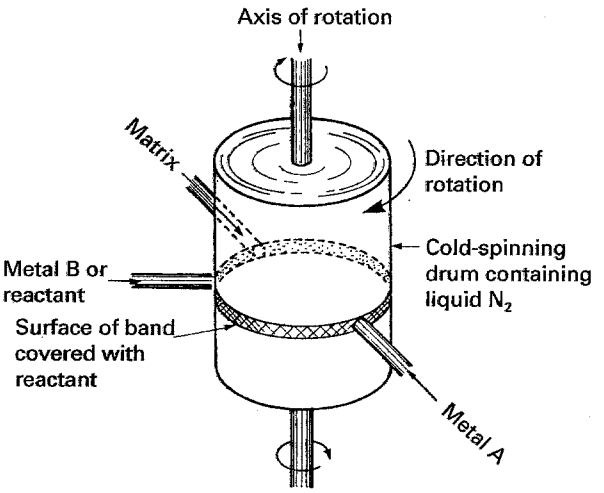

Figure 1 Principles of the rotating cryostat.

Alumina and fumed silica particles were used (particle sizes, 0.03 and 0.014 μm; surface areas 80 and 200 $m^2 g^{-1}$; pore volumes 1 and 0.5 ml g^{-1}, respectively).

2.2.2. Copper carbonyls in adamantane

Similar copper and adamantane deposition and annealing procedures were used but a major modification was the deposition of carbon monoxide in amounts equivalent to three monolayers per revolution, with the CO jet being located between the adamantane jet and the copper furnace. The deposit was a red–purple colour which was indicative of the formation of the copper carbonyls $Cu(CO)_3$ and $Cu_2(CO)_6$ [17, 18]. Their presence, as before, was unequivocally confirmed by infrared, UV/visible and EPR examination of the deposits [17, 18]. They have been observed previously but at much lower temperatures, by Ogden [19], Huber *et al.* [20] and by Kasai and Jones [21]. They are stable in adamantane up to 273 K.

During the annealing and dissolution stage at 110 K, as the adamantane dissolved in the isopentane,

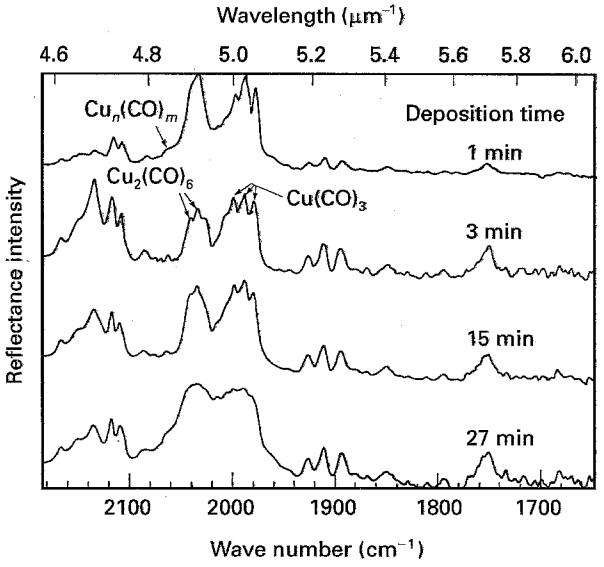

Figure 2 In situ FT–IR spectrum of deposits containing $CuCO_3$, and $Cu_2(CO)_6$, in adamantane prior to transfer to isopentane.

we observed that the isopentane solution developed the characteristic red–purple colour of the copper carbonyl complexes, i.e. they were stable and soluble in isopentane. This colour persisted in the isopentane support slurry even at 193 K but was slowly lost at 273 K to leave a grey-brown coloured support settling out of a clear isopentane solution when no longer agitated.

In the rotating cryostat preparations, we have found it useful to be able to monitor and to control the species present in the deposit by direct *in situ* reflectance infrared and UV/visible spectroscopy during the whole course of the preparation [17, 18]. Fig. 2 shows reflectance FT–IR spectra of the Cu/CO preparations where the distinct bands of $Cu(CO)_3$, $Cu_2(CO)_6$ and $Cu_n(CO)_m$, $n > 2$, $m > 6$, are evident at different deposition times.

It is worth emphasizing the very low temperatures (110–200 K) at which the copper carbonyls decompose and at which the copper crystallites were incorporated into the Al_2O_3 and SiO_2 supports. This minimizes the formation of catalytically ineffective large metal aggregates and crystallites. The sintering problems resulting from the need to use much higher temperatures to decompose the carbonyls of metals such as nickel, rhodium and osmium (see, for example [22, 23]) are obviated, as are those which occur when temperatures of 473–573 K are used to reduce metal oxides with hydrogen or CO after calcination of oxide precursors incorporated into the supports by the conventional catalyst preparation procedures of impregnation and ion-exchange [24].

2.2.3. Direct implantation of copper atoms into sodium chloride supports

Sodium chloride was evaporated directly on to the cooled spinning surface before the deposition of the copper vapour: 1 g sodium chloride and 24 mg copper were deposited in 15 min to give a reddish brown material. We have already shown by EPR that coinage metal atoms can be trapped and small metal crystallites kept in isolation at temperatures well

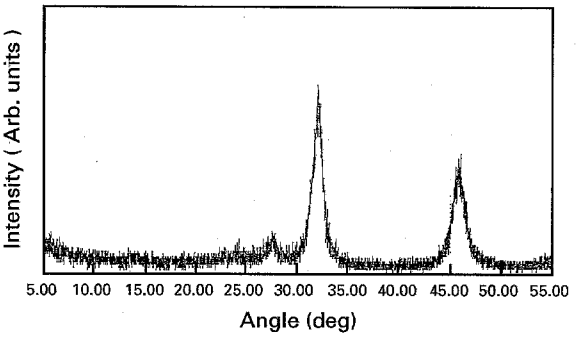

Figure 3 XRD spectrum of NaCl containing copper atoms and clusters.

above 273 K in vapour-deposited alkali-metal chlorides [25]. (The atoms and clusters are located in asymmetric sites at the interfaces between successive chloride layers. The XRD diffraction pattern of the deposits, Fig. 3, recorded at 77 K has distinct reflections at 31° and 45.3° (CuK_α) characteristic of polycrystalline not amorphous NaCl and application of the Scherrer equation to the line widths leads to an average crystallite size of less than 8 nm. Scanning electron micrographs of the NaCl deposits at 298 K also show tightly packed sheets and fibrils of these dimensions in a friable solid, see Fig. 4. These rapidly quenched solids are good examples of alkali halide nanoclusters which are now being widely investigated [26].) In related experiments, Mile *et al.* [5, 27] have trapped organic vapours and metal carbonyls in salt matrices and the salt/molecule technique has been used to prepare unusual anionic species [28, 29].

2.2.4. Preparation of comparison conventional copper catalysts

Comparison was made with copper catalysts. (A) and (B), with similar metal loadings on the same supports which were prepared by conventional methods involving impregnation of the supports with $Cu(NO_3)_2$ solutions, drying at 393 K, calcining at 523 K followed, by reduction with hydrogen at 573 K and reoxidation with oxygen at 653 K [24].

2.3. Activation of copper catalysts

All the Al_2O_3 and SiO_2 supported catalysts were activated by heating in oxygen for 3 h at 753 K to convert the copper completely into CuO. The alkali halide supported catalysts were activated at 373 K for 8 h because sintering occurred above 473 K.

2.4. Determination of catalytic activity

The oxidation of CO to CO_2 by molecular oxygen was chosen as the test reaction for most of the studies because of its simplicity (only one product is possible), and ease of analyses. We used a grease-free, stainless steel/silica apparatus with gas recirculation using a vacuum diaphragm pump and a catalyst bed held on a coarse sinter in a vertical silica reactor (for details see [30]). The bed temperature was measured and

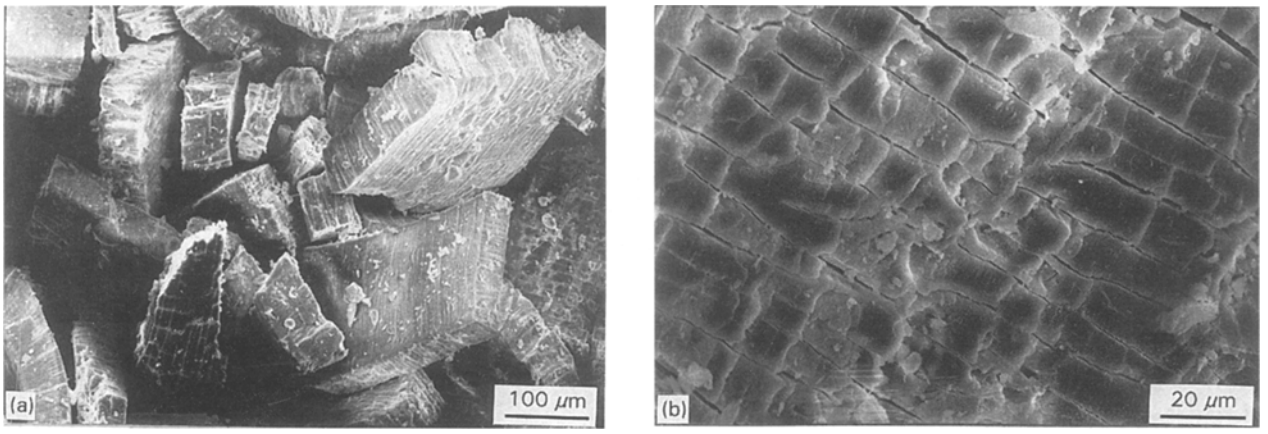

Figure 4 (a, b) Scanning electron micrographs of NaCl chloride deposits prepared on the rotating cryostat.

controlled by a chrome–alumel thermocouple in conjunction with a proportional integral controller supplying power to the furnace surrounding the reactor. The course of the reaction with time was monitored by pressure changes measured on an Omega pressure transducer and by intermittent sampling directly into a Varian 6000 GC through an evacuable six-port valve. A 5 ft (~152.4 cm) carbosieve S-II (1.8 in (~4.57 cm) o.d.) column was used for both activity and N_2O measurements. An overall pressure in the reactor of 760 torr with a $CO:O_2$ ratio of 1:2 was normally used.

We have also made preliminary studies of the methanol and hydrocarbon production from 1:1 mixtures of carbon monoxide and hydrogen at moderately high pressures (30 atm) at 423 K. For this, a Chemical Data System 804 Microreactor Plant Reaction system was used. Runs were at 30 atm of a 1:1 mixture at 423 K flowing continuously at 60 ml min^{-1} through a 25–35 mg catalyst bed. A 12 ft (~366 cm) Poropak R column was used together with flame ionization detector (FID) or thermal conductivity (TC) detection and electronic integration of peak areas using a Spectra Physics computing integrator.

It is important to note that unmodified copper catalysts were examined to enable the most direct and simple comparisons of the catalysts prepared using the rotating cryostat to be made with those prepared by conventional methods. Commercially, promoters and stabilizers such as ZnO and alkali salts are added to enhance catalytic activity, durability and selectivity. Such modifiers could be readily incorporated into the catalysts prepared by the rotating cryostat technique, because they can be introduced continuously into the accumulated molecular layers via the dozen remaining jet ports in the housing of the cryostat.

2.5. Other characterizing techniques

As already mentioned, the processes occurring on the drum and during annealing could be monitored by changes in the infrared and UV–visible spectra at each stage. The supported metal catalysts were also examined by electron spin resonance (ESR), SEM, TEM with electron energy loss spectroscopy (EELS), XRD and X-ray fluorescence in conjunction with SEM. The nitrous oxide method [31] was used to estimate the number of surface copperatoms and hence the dispersion of the copper crystallites (ratio of copper atoms at the surface to the total number of copper atoms in the sample). As already discussed, the broadening of the XRD reflections was also used to estimate the size of the sodium chloride nanocrystallites formed by rapid and continuous quenching of the halide vapour on to the frozen solid surfaces of a halide layer at 77 K.

3. Results

3.1. Particle dispersion and size

3.1.1. Copper cluster- and carbonyl-based catalysts

The dispersion of the copper cluster-based catalysts, as determined by the N_2O method, was 0.5 on Al_2O_3 and 0.75 on SiO_2. This was lower than values close to unity for copper carbonyl-based catalysts on both alumina and silica supports. These dispersions were, however, significantly higher than "conventional" copper catalysts that had values between 0.1 (17% Cu on Al_2O_3) and 0.35 (4.4% Cu on SiO_2).

SEM examination of the samples shown in Tables I and II, together with X-ray fluorescence analysis of local concentrations of copper showed a much more uniform distribution of copper in the cryostatically prepared samples compared with the conventionally prepared catalysts. SEM also revealed a better distribution of copper in the cryostat samples. Fig. 5 shows a subtraction of the EELS images of a $Cu/CO/Al_2O_3$ (CO1) 8.1% Cu on Al_2O_3 8.2% Cu catalyst taken on a Zeiss EM 902 microscope. The bright areas are copper particles ranging in size from 2–10 nm. The near unit dispersion found for the catalysts prepared by the carbonyl route suggests that the copper particles are rafts or monolayer coatings rather than "spherical" or hemispherical particles, because such geometries in this size range would give dispersions of only 0.1–0.3.

3.1.2. Copper in NaCl

XRD and SEM showed that the sodium chloride formed by rigid condensation of NaCl vapour on to

TABLE I Comparison of SiO_2 and Al_2O_3-supported copper catalysts prepared from copper clusters (C1 and C2) generated on the rotating cryostat and those prepared conventionally (A and B)

Catalyst	Temp. (K)	Dispersion	Specific activity (mol CO_2 min^{-1} g^{-1} Cu)	Relative activity[a]
Novel catalyst	393	0.75	$4.0 \pm 0.1 \times 10^{-3}$	80
Cu 7.0%/Al_2O_3 (C1)	423	0.75	$1.0 \pm 0.3 \times 10^{-2}$	200
Novel catalyst	423	NA	$3.0 \pm 0.2 \times 10^{-5}$	6
Cu 5.2%/SiO_2 (C2)	473	NA	$5.0 \pm 0.1 \times 10^{-3}$	100
Comparative catalyst	423	0.3	$2.2 \pm 0.2 \times 10^{-4}$	4
Cu 9.6%/Al_2O_3 (A1)	473	0.3	$2.1 \pm 0.1 \times 10^{-3}$	42
Comparative catalyst	423	0.1	$1.3 \pm 0.1 \times 10^{-4}$	3
Cu 17%/Al_2O_3 (A2)	473	0.1	$1.3 \pm 0.1 \times 10^{-3}$	27
Comparative catalyst	423	0.35	$5.0 \pm 0.2 \times 10^{-5}$	1
Cu 4.4%/SiO_2 (B)	473	0.35	$1.7 \pm 0.1 \times 10^{-3}$	34

[a]Relative to comparative catalyst B at 423 K.

TABLE II Comparison of SiO_2 and Al_2O_3 supported copper catalysts prepared from copper carbonyls (CO1 and CO2) generated on the rotating cryostat and those prepared conventionally (A and B)

Catalyst	Temp. (K)	Dispersion	Specific activity (mol CO_2 min^{-1} g^{-1} Cu)	Relative activity[a]
Novel catalyst	393	~ 1	$1.0 \pm 0.1 \times 10^{-3}$	21
Cu 8.2%/Al_2O_3 (CO1)	423	~ 1	$2.0 \pm 0.1 \times 10^{-3}$	41
	473	~ 1	$1.1 \pm 0.2 \times 10^{-2}$	224
Novel catalyst	423	~ 1	$8 \pm 0.2 \times 10^{-4}$	16
Cu 3.4%/SiO_2 (CO2)	473	~ 1	$9.9 \pm 0.1 \times 10^{-3}$	198
Comparative catalyst	423	0.3	$2.2 \pm 0.2 \times 10^{-4}$	4
Cu 9.6%/Al_2O_3 (A1)	473	0.3	$2.1 \pm 0.1 \times 10^{-3}$	43
Comparative catalyst	423	0.1	$1.3 \pm 0.1 \times 10^{-4}$	3
Cu 17%/Al_2O_3 (A2)	473	0.1	$1.3 \pm 0.1 \times 10^{-3}$	27
Comparative catalyst	423	0.35	$5.0 \pm 0.2 \times 10^{-5}$	1
Cu 4.4%/SiO_2 (B)	473	0.35	$1.7 \pm 0.1 \times 10^{-3}$	34

[a]Relative to comparative catalyst B at 423 K.

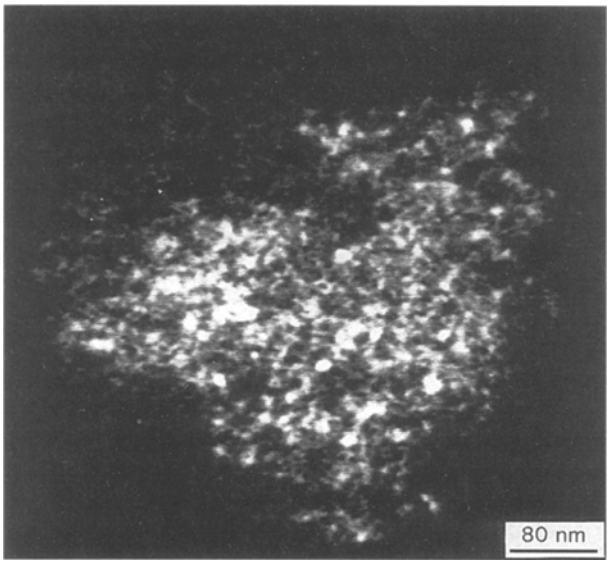

Figure 5 Subtracted EELS images of copper on catalyst CO1.

the 77 K is in the form of nanocrystals (~ 80 nm) in fibrils of $\sim 10^{-7}$ cm diameter. They are microcrystalline not amorphous. The highly fibrous and friable texture of this vapour-deposited salt probably results from the sudden condensation of monolayers of the hot halide vapours on to the previous NaCl clusters held at 77 K. There may be little cohesion between the "new" forming crystalline layer and the "old" previously formed crystalline layers. The copper atoms are trapped in this incoherent layer. Indeed, the EPR transitions from copper atoms trapped in such condensed LiCl, NaCl and KCl matrices have much lower 4s spin densities (<0.5) than gas-phase copper atoms or copper atoms trapped in substitutional sites in single crystals [25]. This is consistent with the copper atoms in the vapour-deposited NaCl being located in asymmetric sites at the interface between the separately deposited layers of NaCl. The asymmetry of these sites results in the admixture of 3d and 4p with 4s orbitals possibly giving rise to dipolar atoms [32]. XPS, XRD and SEM/EELS methods did not reveal copper in these deposits, although a green copper colour could be seen with the naked eye. Either the copper levels (1.5% Cu) in these samples were too low for detection or the copper was located inside the NaCl crystallites beyond the escape depth of a few nanometres. Their dispersion was close to unity, indicating that the N_2O can access these copper nanoclusters if they are so embedded.

TABLE III Comparison of NaCl-supported copper catalysts prepared by direct implantation on the rotating cryostat with those catalysis prepared by conventional routes

Catalyst	Temp (K)	Dispersion	Activity (mol CO_2 min^{-1} g^{-1} Cu)	Relative activity[a]
Novel catalyst	423	1.0	$4.7 \pm 0.1 \times 10^{-4}$	9
Cu 1.5% NaCl	473	1.0	$2.3 \pm 0.2 \times 10^{-2}$	450
Comparative catalyst	423	0.3	$1.3 \pm 0.1 \times 10^{-4}$	4
Cu 9.6%/Al_2O_3 (A1)	473	0.3	$2.1 \pm 0.1 \times 10^{-3}$	42
Comparative catalyst	423	0.35	$5.0 \pm 0.2 \times 10^{-5}$	1
Cu 4.4%/SiO_2 (B)	473	0.35	$1.7 \pm 0.1 \times 10^{-3}$	34

[a]Relative to comparative catalyst B at 423 K.

3.2. Catalytic activity

All catalysts showed good activity for the oxidation of CO to CO_2, $CO + \frac{1}{2}O_2 \rightarrow CO_2$. The specific activities and dispersions of the copper cluster- and the copper carbonyl-based catalysts are listed in Tables I and II, respectively, together with those of the conventionally prepared catalysts. Those prepared by the cryostat technique had significantly higher specific activities at 473 and 423 K on both the Al_2O_3 and SiO_2 supports than analogous catalysts prepared by conventional methods. The maximum relative increase of $\sim$200 at 423 K occurred for catalyst C1 containing 7% Cu on Al_2O_3 prepared from copper clusters. This enhanced activity is also demonstrated by the observation that the conventional alumina-supported catalyst (Al) showed no measurable activity at 393 K while the copper cluster-based catalyst (C1) was 80 times more active at 393 K than the conventional silica catalyst (B1) catalyst at 423 K. Catalyst C1 is so active that at 423 K, thermal runaway of the exothermic reaction soon occurred in the catalyst test rig used.

All Al_2O_3-supported catalysts were more active than their SiO_2-supported counterparts. Surprisingly, despite their slightly higher dispersions ($\sim$1 as opposed to 0.75) produced, the copper carbonyl-based catalysts (CO1 and CO2) did not give the most active catalysts. While the 8.2% copper carbonyl-based Al_2O_3 catalyst CO was 40-fold more active than for conventional silica supported catalyst (B) at 423 K, the 7% copper cluster-based catalyst supported on alumina was more active by a factor 200. The increased activity of the cryostat catalysts on the same support are usually greater than the increase in dispersion by factors of 2–3. Previous studies of the oxidation of CO suggest a structure-insensitive reaction [33, 34] but these small 2–3 enhancements do not merit further speculation at this stage about a change in the demands of the reaction at small dimensions. However, a 50-fold enhancement of the 7% Cu cluster catalyst (C1) on Al_2O_3 over a comparable conventionally based 9.6% Cu on alumina catalyst (A2) does suggest that further careful studies of the structure sensitivity of CO oxidation on such small copper crystallites is warranted. Arrhenius activation energies of about 80 ± 15 kJ mol^{-1} were estimated for all the catalysts, whether prepared conventionally or using the rotating cryostat and accord with previous estimates [33, 34]. The increase in activity of the cryostat-based catalysts appears to be associated with an increased pre-exponential or accessibility factor.

We have demonstrated that active catalysts can be prepared from labile copper clustering, Cu_n and carbonyls $Cu_n(CO)_m$, using cryochemical techniques. They are also durable at moderate temperatures showing no loss of activity over several days at 473 K. However, activity was completely lost after 3 h at 753 K.

3.3. Sodium chloride-supported copper particles

As shown in Table III, these were amongst the most active catalysts prepared in this work but they deactivate above 473 K, a temperature about 40% of the melting point of NaCl (1074 K) and in the region of the anticipated Taman temperature for diffusion. The high activity of this catalyst shows that ingress of reactant gases and exit of the product gases to and from the copper particles embedded in the NaCl nanocrystals readily occurs. These catalysts are probably of little commercial value because of their low durability, the volatility of NaCl and problems of handling such fine powders in industrial reactors. However, such small nanocrystals of alkali salts could have applications in making semipermeable membranes by incorporating them into polymer melts followed by their aqueous dissolution to leave behind a network of porous structures. Their high surface area could also be useful for nucleophilic halogen exchange as demonstrated by Whyman *et al.* [35].

3.4. Preliminary studies of the hydrogenation and oligomerization of CO/H_2 mixtures at 30 atm

Only a few experiments have been carried out on these reactions but the results are sufficiently interesting to be reported here. Alcohol, alkane and alkene formation was observed for the copper cluster catalyst (C1) and the conventional catalyst (A1) supported on γ-alumina, but minimal reaction occurred on silica-supported catalysts. Table IV compares the rates of

TABLE IV CO/H_2 catalysed reactions at 30 atm and 523 K

Catalyst	Rate selectivity (%)						
	(10^3 mol $CO\,min^{-1}\,g^{-1}$ Cu)	CH_4	$\Sigma_i C_i^{+a}$	CH_3OH	C_2H_5OH	C_2/C_2^b	C_3/C_3^b
Novel catalyst Cu 8.2%, Al_2O_3 (C1)	4.8	18	67	12	3	1.3	3.5
Comparative catalyst Cu 9.6%, Al_2O_3 (A1)	1.3	37	37	20	6	0.26	1.15

[a]Summation of hydrocarbons above C_2.
[b]Alkene to alkane ratio.

conversion of CO into these products and the selectivities at 30 atm and 523 K in the Chemical Data System microreactor. Only traces of alcohols above C2 and hydrocarbons above C3 were detected. The overall rate on catalyst (C1) was five times higher than on the conventional catalyst (A1) but this arises mainly from its dispersion (0.75 compared with 0.3). Nevertheless, there are major differences in the product distributions or selectivities on the two catalysts. There is a small shift towards hydrocarbons (85% on C1, 74% on A1) over alcohols but the major change is the much higher yields of the C2 and C3 yields and lowering in CH_4 on the cryostat-based catalyst. The alkene to alkane ratio is also three to five times higher than from catalyst A1. It appears from these preliminary results that the chemistry of CO/H_2 is significantly different on the cryostat catalysts. We are encouraged by these early results but a full investigation needs to be undertaken before a detailed mechanistic interpretation is warranted.

4. Conclusions

1. Three new methods of making supported copper catalysts based on the rotating cryostat technique are described and their catalytic activities and other characteristics determined.

2. Two methods exploit previous findings of the "stability" of copper carbonyls $Cu_n(Cu)_m$ ($n = 1$ or 2, $m = 1$–6) and small clusters Cu_n ($n > 3$) in an adamantane matrix up to temperatures of 222 K. The catalysts were prepared by slowly dissolving the adamantane in isopentane containing slurries of either Al_2O_3 or SiO_2 at the melting point of isopentane.

3. The catalysts so prepared contain very small copper particles (≤ 8 nm) with dispersions close to unity.

4. Their activity for the oxidation of CO to CO_2 can be orders of magnitude higher than that of similar catalysts prepared by conventional methods.

5. They are durable up to 473 K.

6. The third method involves the direct implantation of copper atoms from the vapour phase into NaCl nanocrystals (< 8 nm) prepared by a previous rapid condensation of NaCl vapour.

7. Cu/NaCl catalysts are active for CO oxidation but are not durable above 423 K.

8. All three catalyst systems are more active than conventional copper catalysts for the conversion of Cu/H_2 into alcohols, alkanes and alkenes at 30 atm and 573 K.

Acknowledgements

We thank our colleagues in NRC for their help with the following aspects: D. F. Mitchell and P. T. Robinson, TEM and EELS; T. Quinn, SEM; J. S. Tse, XRD and XPS; D. Klug, FT–IR.

References

1. K. J. KLABUNDE, H. F. EFNER, L. SATEK and J. J. DONLEY, *Organomet. Chem.* **71** (1974) 309.
2. S. C. DAVIS and K. J. KLABUNDE, *Chem. Rev.* **82** (1982) 153.
3. B. J. TAN, K. J. KLABUNDE, T. TANAKA, H. KANAI and S. YOSHIDA, *J. Am. Chem. Soc.* **110** (1988) 5951.
4. L. F. NAZAR, G. A. OZIN, F. HUGHES, J. GODBER and D. RANCOURT, *Angew. Chem. Suppl.* (1983) 898.
5. G. A. OZIN and M. P. A. ANDREWS, in "Metal Clusters in Catalysis", Studies in Surface Science and Catalysis, Vol. 28, edited by B. C. Gates, L. Guczi and H. Knozinger (Elsevier, Amsterdam, 1987) p. 265.
6. G. A. OZIN, R. A. PROKOPOWICZ, H. X. STUBER and D. HADDLETON, in "Leo Friend Symposium", Division of Industrial and Engineering Chemistry, 196th American Chemical Society Meeting, Los Angeles, September 1988.
7. J. P. CANDLIN, UK Pat. 48406/75 (1975).
8. G. A. OZIN, *J. Am. Chem. Soc.* **102** (1980) 3301.
9. R. N. EDMONDS, M. R. HARRISON and P. P. EDWARDS, *Ann. Rep. Prog. Chem. Sect. C* **82** (1985) 205.
10. K. L. CHOPRA, "Thin Film Phenomena" (McGraw Hill, New York, 1974).
11. J. R. ANDERSON and N. R. AVERY, *J. Catal.* **5** (1966) 446.
12. J. E. BENNETT, B. MILE, A. THOMAS and B. WARD, *Adv. Phys. Org. Chem.* **8** (1970) 1.
13. A. J. BUCK, J. A. HOWARD and B. MILE, *J. Am. Chem. Soc.* **105** (1983) 3381.
14. J. A. HOWARD and B. MILE, *Acc. Chem. Res.* **20** (1987) 173.
15. *Idem, Electron Spin Reson.* **11B** (1989) 136.
16. B. MILE, J. A. HOWARD, M. HISTED, H. MORRIS and C. A. HAMPSON, *Farad. Discuss.* **92** (1991) 129.
17. J. A. HOWARD, B. MILE, J. R. MORTON and K. F. PRESON, *J. Phys. Chem.* **90** (1986) 1033.
18. J. H. B. CHENIER, C. A. HAMPSON, J. A. HOWARD and B. MILE, *J. Phys. Chem.* **93** (1989) 114.
19. J. S. OGDEN, *J. Chem. Soc. Chem. Commun.* (1981) 978.
20. H. HUBER, E. P. KUNDIG, M. MOSKOVITS and G. A. OZIN, *J. Am. Chem. Soc.* **97** (1975) 2097.
21. P. H. KASAI and P. M. JONES, *ibid.* **107** (1985) 803.
22. R. PSARO and R. UGO, in "Metal Clusters in Catalysis", Studies in Surface Science, Vol. 28, edited by B. C. Gates, L. Guczi and H. Knozinger (Elsevier, Amsterdam, 1987) p. 427.

23. B. C. GATES, L. GUCZI and H. KNOZINGER, *ibid.* p. 607.
24. B. MILE, D. STIRLING, M. A. ZAMMITT, A. LOVELL and M. WEBB, *J. Catal.* **114** (1988) 217.
25. J. H. B. CHENIER, J. A. HOWARD, H. A. JOLY and B. MILE, *J. Chem. Soc. Chem. Commun.* **86** (1990) 2169.
26. R. L. WHETTEN, *Acc. Chem. Res.* 26 (1993) 49.
27. J. H. HOWARD, H. DAHMANE, B. MILE and R. SUTCLIFFE, *J. Chem. Soc.* (1983) 1068.
28. R. S. AULT, *Inorg. Chem.* **22** (1983) 2221.
29. E. KIRKOR, J. GEBICKY, D. R. PHILLIPS and J. MICHL, *J. Am. Chem. Soc.* **108** (1986) 7106.
30. Y. AMENOMYA, *J. Catal.* **55** (1978) 212.
31. F. S. STONE, *Adv. Catal.* **13** (1962) 1.
32. D. E. LOGAN, *J. Chem. Phys.* **86** (1987) 234.
33. T. ENGEL and G. ERTLE, *Adv. Catal.* **28** (1979) 1.
34. R. WHYMAN, R. L. POWELL and J. H. CLARK, in "Leo Friend Symposium", Division of Industrial and Engineering Chemistry, 196th American Chemical Society Meeting, Los Angeles, September 1988.

Received 10 August
and accepted 8 September 1995